Influence of distinct kinds of temporal disorder in discontinuous phase transitions

Jesus M. Encinas ⬤ and C. E. Fiore ⬤ *

Instituto de Física, Universidade de São Paulo, Caixa Postal 66318 05315-970 São Paulo, São Paulo, Brazil

Based on mean-field theory (MFT) arguments, a general description for discontinuous phase transitions in the presence of temporal disorder is considered. Our analysis extends the recent findings [C. E. Fiore *et al.*, Phys. Rev. E **98**, 032129 (2018)] by considering discontinuous phase transitions beyond those with a single absorbing state. The theory is exemplified in one of the simplest (nonequilibrium) order-disorder (discontinuous) phase transitions with "up-down" Z_2 symmetry: the inertial majority vote model for two kinds of temporal disorder. As for absorbing phase transitions, the temporal disorder does not suppress the occurrence of discontinuous phase transitions, but remarkable differences emerge when compared with the pure (disorderless) case. A comparison between the distinct kinds of temporal disorder is also performed beyond the MFT for random-regular complex topologies. Our work paves the way for the study of a generic discontinuous phase transition under the influence of an arbitrary kind of temporal disorder.

I. INTRODUCTION

Disorder is commonly present in many real systems and more recently it has also been broadly investigated in nonequilibrium phase transitions with absorbing states [1–3] by considering spatial [4–8] and temporal [9–17] variation of control parameters. In both cases, the criticality is marked by the existence of new (and universal) set of critical exponents and present a subregion in the phase space in which exotic behaviors are found. The former region is named spatial Griffiths phase and it is located in the absorbing phase in which the order parameter vanishes slower (power law or stretched exponential) than the exponential decay in the absence of disorder. Conversely, temporal disorder is featured by a region in the active phase in which the mean lifetime increases as a power law (instead of exponential).

Now let us shift the discussion for nonequilibrium phase transitions with spontaneous breaking symmetry. It manifests in a countless sort of systems beyond the classical ferromagnetic-paramagnetic phase transition [1,2,18], such as for an (approximate) description for fish shoals moving under an ordered way for protecting themselves against predators, spontaneous formations of a common language and culture, the emergence of consensus in social systems, and others [19–21]. They can be qualitatively expressed via the differential equation for the order-parameter x $dx/dt = ax + bx^3 - cx^5 \dots$. It presents only odd terms, in which the classification of phase transition, whether continuous or discontinuous, depends on the above coefficients (b and c should be positive for a discontinuous phase transition). Despite predicted under the simple above approach, comparatively there are less (nonequilibrium) microscopic models presenting discontinuous transitions exhibiting up-down symmetry. A remarkable example is the majority vote model with inertia [22]. Originally, its phase transition is always

continuous [23–25], but the inclusion of an inertial term, e.g., a term proportional to the local spin, can shift the phase transition to a discontinuous one, in both complex network [22,26] and in regular lattices [27,28].

The importance of such results is highlighted not only for occurrence of discontinuous phase transition in a minimal nonequilibrium model in which general features at the phase coexistence were established [27,28], but also by the fact that behavioral inertia is an essential characteristic of human being and animal groups and it is also a significant ingredient triggering abrupt transitions arising in social systems [19]. Thereby, the inertial majority vote (IMV) could be (in principle) considered for the description of such phenomena. However, the effects under the inclusion of more realistic ingredients, such as its time dependent variation of parameters (e.g., inertia), have not been satisfactorily understood yet.

Recently, a theory for discontinuous phase transitions with a single absorbing state in the presence of temporal disorder was proposed in Ref. [29]. In contrast to the spatial disorder case [30], they are not suppressed due to the temporal disorder, although remarkable features emerge when compared with their pure (disorderless) systems. This includes the existence of rare temporal fluctuations which changes the behavior of metastable phase, turning it into an inactive phase characterized by exponentially large decay times. Since systems with Z_2 symmetry present distinct features from phase transitions into a single absorbing state (which can be viewed by a distinct differential equation $dx/dt = ax + bx^2 - cx^3 \dots$) [31,32], a question that naturally arises is if similar findings about the effect of temporal disorder are verified and can be extended beyond Ref. [29]. Due to the fact that inertia plays a fundamental role for shifting the phase transition in the IMV, an interesting question concerns that temporal disorder in the inertia may provide similar findings to the usual case (temporal disorder in the control parameter).

Aimed at answering aforementioned points, here we examine, separately, the role of temporal disorder in two

―――――――
*fiorecarlos.cf@gmail.com

fundamental ingredients: the control parameter and inertia. Based on mean-field analysis, we derive general predictions for both kinds of temporal disorder, which are also verified beyond the mean-field theory (MFT) for complex structures. Our analysis provides a general procedure for tackling the effect of temporal disorder in discontinuous phase transitions.

This paper is organized as follows: In Sec. II we present the analysis of pure model and temporal disorder based on the MFT, and in Sec. III we present the main findings beyond the MFT. Conclusions are drawn in Sec. IV.

II. MODEL AND MEAN-FIELD ANALYSIS

The original (inertialess) majority vote model (MV) is defined as follows. At each time step, a site i with spin σ_i is randomly selected and with probability $1 - f(f)$ it is (is not) aligned with the majority of its k_i nearest neighbors. If there is no majority of a given spin (whether $+1$ or -1), one of the possible values is chosen with equal probability. The inertial majority vote model (IMV) differs from the MV by the inclusion of an inertial term θ, taking into account the contribution of the local spin. The transition rate $\omega_i(\sigma)$ associated to the spin flip $\sigma_i \rightarrow -\sigma_i$ also depends on the local spin σ_i and it is given by [22]

$$\omega_i(\sigma) = \frac{1}{2}[1 - (1 - 2f)\sigma_i S(\Theta_i)], \quad (1)$$

where Θ_i accounts for the local neighborhood plus the inertial contribution given by

$$\Theta_i = (1 - \theta) \sum_{j=1}^{k_i} \frac{\sigma_j}{k_i} + \theta \sigma_i,$$

with $S(x) = \text{sign}(x)$ if $x \neq 0$ and $S(0) = 0$. Note that one recovers the original MV when $\theta = 0$. Except to the trivial cases, $f = 0$ and $\theta = 0.5$, there is (always) a finite probability of not following the majority vote rule and hence the phase transition does not present an absorbing phase [29]. An order-disorder phase transition yields only when the inertia is constrained between $\theta \in [0, 0.5]$. For $\theta > 0.5$ there is no interaction between neighboring sites and the transition rate is always dominated by the inertial term. Since spin flips

due to the interaction between neighboring spins are absent, there is neither spontaneous magnetization nor phase transition. By increasing θ and the connectivity, phase transition is shifted from continuous (second order) to a discontinuous (first order). At the mean-field level the phase coexistence is marked by the appearance of an hysteretic region in which two symmetric ordered phases and a disordered phase coexist. A discontinuous phase transition also manifests in homogeneous and heterogeneous networks, but an entirely different behavior is presented for regular lattices, in which the main quantities (magnetization, its variance χ, the entropy production, the position of maximum of χ) scale with the system volume at the phase coexistence [27,28,33].

From the transition rate, the time evolution of the average magnetization $m_k = \langle \sigma_i \rangle_k$ of a local site i with degree k is given by

$$\frac{d}{dt} m_k = -m_k + (1 - 2f)\langle S(\Theta_i) \rangle. \quad (2)$$

The first analysis will be performed by means of a MFT treatment, in which the joint probabilities appearing in the average $\langle S(\Theta_i) \rangle$ are rewritten in terms of one-site probabilities. From this assumption, one gets the following expression $\langle S(\Theta_i) \rangle = (1 + m_k)\langle S(\Theta_+) \rangle / 2 + (1 - m_k)\langle S(\Theta_-) \rangle / 2$, where $\langle S(\Theta_\pm) \rangle$ are given by

$$\langle S(\Theta_\pm) \rangle \approx \sum_{n=\lceil n_k^\pm \rceil}^{k} C_n^k p_+^n p_-^{k-n} - \sum_{n=\lceil n_k^\mp \rceil}^{k} C_n^k p_-^n p_+^{k-n}, \quad (3)$$

with $p_\pm$ being the probability of a nearest neighbor having spin ± 1 given by $p_\pm = (1 \pm m^*)/2$ (associated with the "local" magnetization m^*), n_k^- and n_k^+ correspond to the lower limit of the ceiling function given by $n_k^- = k/[2(1 - \theta)]$ and $n_k^+ = k(1 - 2\theta)/[2(1 - \theta)]$, respectively.

In order to relate m^* and m_k, we shall focus our analysis on uncorrelated networks, in which the probability of a randomly chosen site has degree k reads as $kP(k)/\langle k \rangle$, with $P(k)$ and $\langle k \rangle$ being the probability distribution of nodes and its mean degree, respectively. The relation between m^* and m_k then reads as $m^* = \sum_k m_k kP(k)/\langle k \rangle$. By combining the above expression with Eq. (2), we obtain the following equation of m^* in the steady-state regime:

$$m^* = (1 - 2f) \sum_k \frac{kP(k)}{\langle k \rangle} \left[\left(\frac{1 + m_k}{2} \right) \langle S(\Theta_+) \rangle + \left(\frac{1 - m_k}{2} \right) \langle S(\Theta_-) \rangle \right]. \quad (4)$$

Equation (4) can be analyzed for a generic lattice topology [specified by $P(k)$]. We restrict our study for random-regular (RR) topologies, in which all sites have the same number of neighbors k_0 [$P(k) = \delta(k - k_0)$] and one gets the following self-consistent expression for the steady m in terms of f and θ:

$$m = (1 - 2f) \left[\left(\frac{1 + m}{2} \right) \langle S(\Theta_+) \rangle + \left(\frac{1 - m}{2} \right) \langle S(\Theta_-) \rangle \right], \quad (5)$$

where we considered the fact that $m^* = m$. Equation (5) presents three steady-state solutions $m_s(f) > m_u(f) > m_d(f) = 0$ and a discontinuous phase transition occurring at $f = f_f$. For $f > f_f$, the system evolves to the solution $m_d(f) = 0$ for $t \rightarrow \infty$, characterizing the disordered (DIS)

phase irrespective of the initial condition. Conversely, the ordered phase is separated by two distinct regions: $f < f_b$ and $f_b < f < f_f$. In the former, the time evolution of $m(t)$ evolves to $m(t \rightarrow \infty) \rightarrow m_s(f)$, also independently of the initial condition, whereas for $f_b < f < f_f$ the steady

state depends on the initial condition. More specifically, for $m(0) > m_u(f)$ and $m(0) < m_u(f)$ the system will evolve to $m(t \to \infty) \to m_s(f)$ (ordered phase) and $m(t \to \infty) \to m_d(f)$ (disordered phase), respectively. This feature of the ordered phase will be referred as the metastable (ME) phase, contrasting with the behavior for $f < f_b$. The value $f = f_b$ marks the crossover between the above regimes. Since $m(t)$ deviates from $m_u(f)$ whenever $m(0) \neq m_u(f)$, such a solution is unstable.

Although the achievement of analytic expressions for the steady-state regime and transition point from Eqs. (4) and (5) become quite cumbersome as k_0 is raised, a simpler analysis can be performed in the limit of large connectivities since each term of the binomial distribution approaches a Gaussian with mean $k_0 p_\pm$ and variance $\sigma^2 = k_0 p_+ p_-$ [24,26,33–35]. From Eq. (5), each term from the right hand side is approximately rewritten as

$$\sum_{n=\lceil n_k^\pm \rceil}^{k_0} C_n^{k_0} p_\pm^n p_\mp^{k_0-n} \to \frac{1}{\sigma\sqrt{2\pi}} \int_{n_k^\pm}^{k_0} e^{-\frac{(\ell - k_0 p_\pm)^2}{2\sigma^2}} d\ell = \frac{1}{2}\sqrt{\pi}\left\{ \mathrm{erf}\left[\frac{k_0(1-p_\pm)}{\sqrt{2}\sigma}\right] - \mathrm{erf}\left[\frac{k_0(n_k^\pm - p_\pm)}{\sqrt{2}\sigma}\right]\right\}, \tag{6}$$

with erf(x) denoting the error function $\mathrm{erf}(x) = 2\int_0^x e^{-t^2} dt/\sqrt{\pi}$, and the second one can be rewritten under a similar way. Taking into account that $\mathrm{erf}[k_0(1 - p_\pm)/\sqrt{2}\sigma]$ approaches to 1 for large k_0, we arrive at the following expression for the steady-state regime:

$$f = \frac{1}{2}\left[1 - \frac{2m}{(1+m)\mathrm{erf}(\alpha) - (1-m)\mathrm{erf}(\beta)}\right], \tag{7}$$

where parameters α and β are given by

$$\alpha = \sqrt{\frac{k_0}{2}}\left[\frac{\theta}{1-\theta} + m\right] \quad \text{and} \quad \beta = \sqrt{\frac{k_0}{2}}\left[\frac{\theta}{1-\theta} - m\right], \tag{8}$$

respectively. The transition point f_f corresponds to the maximum of Eq. (7), whereas at the vicinity of f_b (or f_c for a critical phase transition), m is expected to be small and then the above differential equation approaches $dm/dt \approx A(f, \theta, k_0)m$, where $A(f, \theta, k_0)$ is given by

$$A(f, \theta, k_0) = -1 + (1 - 2f)\left[\sqrt{\frac{2k_0}{\pi}}e^{-\frac{k_0\theta^2}{2(1-\theta)^2}} + \mathrm{erf}\left(\sqrt{\frac{k_0}{2}}\frac{\theta}{1-\theta}\right)\right]. \tag{9}$$

From the above expression, f_b is then given by $A(f_b, \theta, k_0) = 0$ and marks, for a given value of θ, the separatrix between an exponentially growth to the steady-state value $m_s(f)$ if $A(f, k_0, \theta) > 0$ ($f < f_b$) and an exponential decay to $m_d(f)$ if $A(f, k_0, \theta) < 0$ ($f > f_b$). For $\theta = 0$, one recovers the expression for the critical point $2f_c = 1 - \sqrt{\pi/(2k)}$ [24,33].

In order to illustrate all previous findings, Fig. 1 depicts, for the clean system, the phase diagram and all the above main features of discontinuous phase transitions for $k_0 = 12$ and $\theta = 0.45$ as f is changed. In particular, the regions $f \leqslant f_b = 0.027\,4573\ldots$ and $f_b < f < f_f = 0.080\,121$ mark the ordered (ORD) and ME phases, respectively, whereas for $f > f_f$ the disordered phase (DIS) prevails. Similar results are obtained for other connectivities k_0 and θ.

As a final remark, it is worth mentioning that although the dependence between m and θ is more cumbersome than with f, all previous signatures of phase coexistence are held valid when the inertia is taken as the control parameter (for fixed f).

A. Temporal disorder in the control parameter

Once we presented the main features about the pure system, we now are in position for tackling the effects of the temporal disorder. We start with time variations of the control parameter f. Although similar findings are expected for

distinct temporal disorder distributions, we shall consider the simplest case in which for a given time interval constrained between t and $t + \Delta t$, control parameter f is randomly extracted from a bimodal distribution $P_{\mathrm{dis}}(f)$:

$$P_{\mathrm{dis}}(f) = p\delta(f - f_-) + (1 - p)\delta(f - f_+), \tag{10}$$

where $f_- < f_+$ and $p(1 - p)$ is the probability in which f assumes the values $f_-(f_+)$. During this time interval, the system behaves as the pure system since its control parameter is kept fixed. For simplicity and also for comparing with previous findings [29], we set $p = \frac{1}{2}$.

Analysis starts from a given initial condition $m(0)$ and its time evolution is analyzed until a sufficient large time $t_{\max}$ that generates a given sequence of control parameter values $\{f_1, f_2, \ldots, f_M\}$, where $t_{\max} = M \times \Delta t$. This process is then repeated for sufficiently N_D distinct disorder sequences (we have considered here $N_D = 10^2$–10^3).

Although our findings do not depend on particular values of k_0 and θ, the effect of temporal disorder will be exemplified for $k_0 = 12$ and $\theta = 0.45$, in order to draw a comparison between clean and disordered systems. All possible variations of both f_- and f_+ along ORD, ME, and DIS will be considered. We face two scenarios, in which both f_- and f_+ belong to the same and different phases, respectively.

Let us start with the case when both f_- and f_+ vary over the ordered phase ($0 \leqslant f_\pm < f_b$). Irrespective of the initial
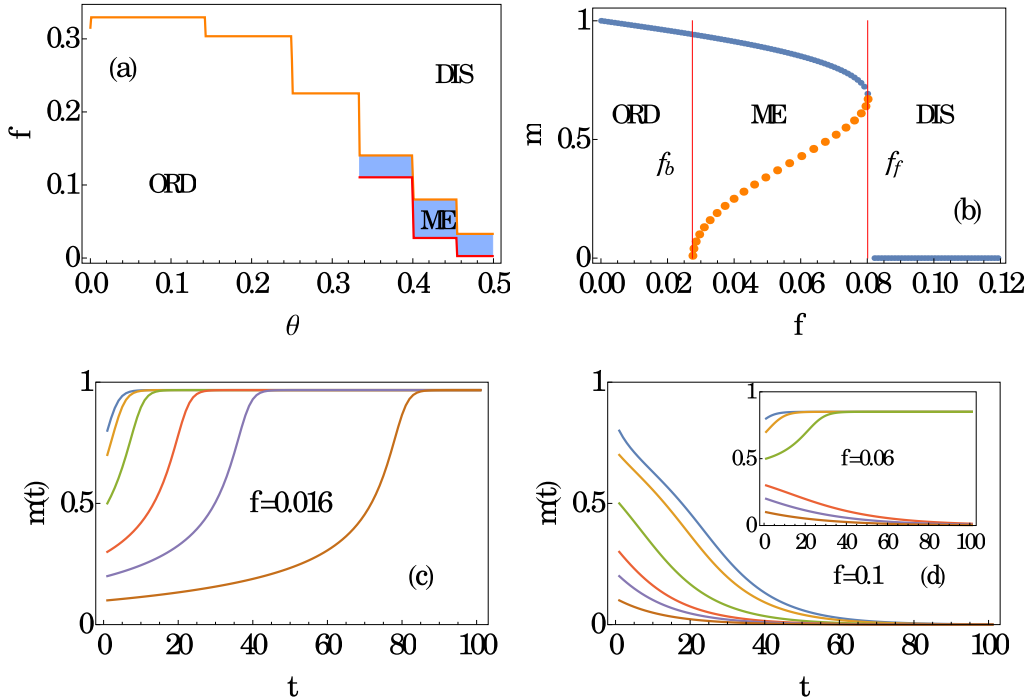
FIG. 1. (a) Depicts the MFT phase diagram for a RR topology with $k_0 = 12$. ORD, ME, and DIS denote the ordered, metastable, and disordered phases, respectively. In (b), the steady magnetization m versus f for $\theta = 0.45$. Continuous and dashed lines denote the stable and unstable solutions of Eq. (5), respectively. Their main features are exemplified in (c) and (d) by taking the time evolution of m as a function of time for $f = 0.016(c)$, $f = 0.10(d)$ and 0.06 (inset) for distinct initial conditions $m(0)$.

condition $m(0)$, the system will evolve towards an ordered state in which the steady magnetization fluctuates between $m_s(f_-)$ and $m_s(f_+)$. A similar conclusion is valid when both f_- and f_+ belong to the disordered phase ($f_f < f_\pm \leqslant \frac{1}{2}$), in which the disordered phase prevails independently of $m(0)$. For both f_- and f_+ belonging to the metastable phase [$f_b \leqslant f_\pm \leqslant f_f$ and $m_u(f_-) < m_u(f_+)$], then $m(t \to \infty) \to 0$ and $m(t \to \infty) \neq 0$ if $m(0) < m_u(f_-)$ and $m(0) > m_u(f_+)$, respectively, irrespective of the sequence of f_- and f_+. The case in which $m_u(f_-) < m(0) < m_u(f_+)$ will depend on the particular sequence of f_- and f_+. This can be verified under two extreme cases. Take, for instance, a particular (long) sequence of $f = f_+$, in which $m(t)$ becomes lower than $m_u(f_-)$. In such a case, the system always reaches the disordered phase. Conversely, a long sequence of $f = f_-$ will lead to $m(t) > m_u(f_+)$ and then the system will converge to the ordered phase. Thus, as for absorbing phase transitions [29], ORD, ME, and DIS phases are preserved under the temporal disorder.

Next, we analyze the cases in which f_- and f_+ belong to different phases. Starting with $f_- \in$ ORD and $f_+ \in$ ME (with $f_- < f_b$ and $f_b < f_+ < f_f$), the phase predominance can be understood under a heuristic analysis based on the time evolution for $m(t) \ll 1$. Since the inertia is fixed, Eq. (9) assumes the form $m \sim e^{-\alpha(f-f_b)t}$, where parameters α and f_b are approximately given by Eq. (9) for large k_0. The dynamics then will be characterized for sequences in which $m(t)$ increases and vanishes according to asymptotic expressions $m \sim e^{\alpha(f_b-f_-)t}$ and $m \sim e^{-\alpha(f_+-f_b)t}$, respectively. The ordered phase prevails if $f_+ + f_- < 2f_b$, whereas the metastable phase dominates when $f_+ + f_- > 2f_b$. The line

fulfilling $f_+ + f_- = 2f_b$ denotes the crossover between ordered and metastable phase lines.

Next, we consider f_- and f_+ belonging to the ME and DIS phases, respectively. Despite different from absorbing phase transitions (APTs) [29], the existence of a hysteretic branch is also responsible for the prevalence of the disordered phase over the metastable one. Since the magnetization vanishes for $f > f_f$, irrespective of the initial condition, it suffices a single long sequence of consecutive f_+'s (e.g., a rare fluctuation) in which $m(t) < m_u(f_-)$ for the system always reaching the disordered phase. For sufficiently long times, a rare fluctuation occurs with probability one and thus the temporal disorder always suppresses the ME phase when $f_+ > f_f$. However, the appearance of a rare fluctuation may require exponentially large times (mainly when f_+ approaches to f_f and/or for small Δt's). The above features are depicted in Fig. 2(d) by comparing the time evolution of the magnetization over individual runs and its average value. Note that in all cases, individual runs are featured by the system evolving to the disordered phase after the appearance of a rare fluctuation. Since the interval time in which it appears varies, individual and averaged runs behave very differently. The latter exhibits a "plateau," reflecting the absence of a rare fluctuation that drives the system to the disordered phase for lower and intermediate times. The plateau is more pronounced for lower time windows Δt and it is followed by the vanishing of the mean magnetization according to a characteristic time $\overline{T}$. In order to obtain an upper limit for $\overline{T}$, we assume the extreme case in which the disordered phase is reached only via a long sequence of consecutive f_+'s, whose magnetization evolves
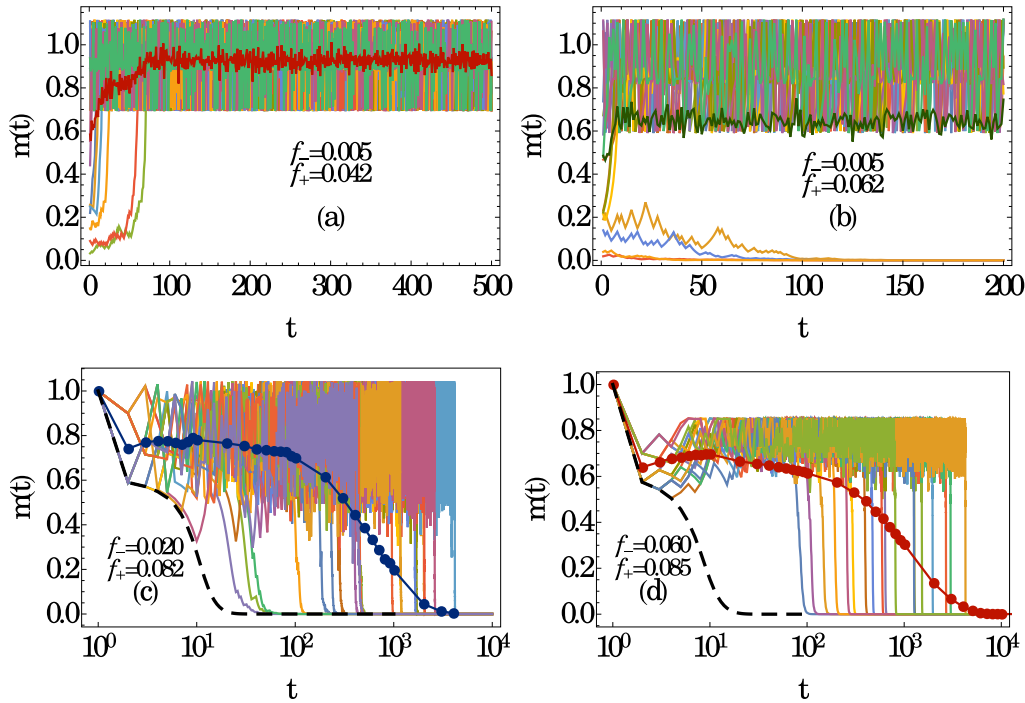
FIG. 2. MFT temporal disorder analysis: For a RR network with $k_0 = 12$, $\theta = 0.45$, and $\Delta t = 5$, the time evolution of m for distinct sets of f_+ and f_- and distinct independent realizations. (a)–(d) Exemplify the following cases: $(f_-, f_+) \in (\text{ORD}, \text{ME})$ with $\bar{f} < f_b$ and $\bar{f} > f_b$, $(f_-, f_+) \in (\text{ORD}, \text{DIS})$, and $(f_-, f_+) \in (\text{ME}, \text{DIS})$, respectively. Dashed and symbol curves correspond to the pure versions (for $f = f_+$) and m averaged over $N_D = 10^3$ realizations, respectively.

from $m_s(f_-)$ to $m_u(f_-)$ (when $f = f_+$) and it is characterized by the decay time τ_+. The mean characteristic time $\overline{T}$ is approximately given by $\overline{T} \approx \tau_+ p^{-\tau_+/\Delta t}$ [29]. Figures 3(a) and 3(b) depict the time evolution of average $m(t)$ for distinct Δt's for $(f_-, f_+) \in (\text{ORD}, \text{DIS})$ and (ME, DIS), respectively. As can be seen, the relationship between $\overline{T}$ and Δt follows rather well such above theoretical estimate. According to it, the appearance of a rare fluctuation driving the system to the disordered phase would require a sufficient long time $\overline{T} \approx 10^{13}$ for $\Delta t = 1$. We close such analysis by remarking that although the disordered phase prevails over the metastable, the discontinuous phase transition between DIS and ME phases is preserved by the temporal disorder and yields at $f_+ = f_f$.

Since the disordered and metastable phases behave similarly when $m(t) \ll 1$, the case in which f_- and f_+ belong to the ORD and DIS phases is similar to the first one and then the ordered and disordered phases prevail if $\bar{f} < f_b$ and $\bar{f} > f_b$, respectively. The relation $2f_b = f_+ + f_-$ marks the separatrix between the above regimes. As previously, the average $m(t)$ is significantly different from individual runs and the mean decay time also increases as Δt decreases. These features are exemplified in Figs. 2(c) and 3(a) for $\Delta t = 5$, $f_- = 0.020$, and $f_+ = 0.082$ with $N_D = 20/10^3$ individual/averaged runs. The prevalence of ORD phase is possible only for smaller values of inertia ($\frac{1}{3} < \theta < \frac{2}{5}$ and $\frac{3}{13} < \theta < \frac{1}{3}$ for $k_0 = 12$ and 20, respectively). In the present case, the phase DIS always dominates over the ORD phase for $k_0 = 12$ and $\theta = 0.45$ since the summation of lowest $f_- = 0$ and $f_+ = f_f$ is always greater than $2f_b$.

From the previous analysis, we build the phase diagram for the temporal disorder IMV for $k_0 = 12$ and $\theta = 0.45$,

as depicted in Fig. 4. Dotted and dashed lines denote the crossover and phase coexistence lines between phases.

We close this section by remarking that although APT and up-down systems share distinct features, the effect of temporal disorder is similar and directly related to the bistability of the active or ordered phase.

B. Temporal disorder in the inertia

Now we consider the effects of temporal disorder in the inertia, in which its values are chosen from two possible values θ_- and θ_+ (with $\theta_+ > \theta_-$):

$$P_{\text{dis}}(\theta) = p\delta(\theta - \theta_-) + (1 - p)\delta(\theta - \theta_+). \quad (11)$$

Although the dependence between the $m(t)$ and θ is more cumbersome than the control parameter f, our analysis will be carried out for $m(t) \ll 1$, in which the time evolution of the order parameter is approximately given by $dm/dt \approx A'(f, \theta, k_0)m$ [the coefficient $A'(f, \theta, k_0)$ approaches to Eq. (9) for large k_0]. Since $A'(f, \theta, k_0) > 0 (< 0)$ for θ belonging to the ORD (ME and DIS) phases [see, e.g., Tables I and II and Eq. (9)], the inertial disorder can be analyzed in similarity with the temporal disorder in f, whose resulting phase is predicted from the competition between $A'(f, \theta_+, k)$ and $A'(f, \theta_-, k)$.

Table I and Fig. 5(d) exemplify coefficients $A'(f, \theta, k_0)$ and the phase diagram for $f = 0.12$ and distinct θ's, respectively. For the pure version, the crossover between ORD and ME phases yields at $\theta_b = \frac{1}{3}$, whereas ME-DIS discontinuous phase transition yields at $\theta_f = \frac{2}{5}$ [see, e.g., Fig. 1(a)].
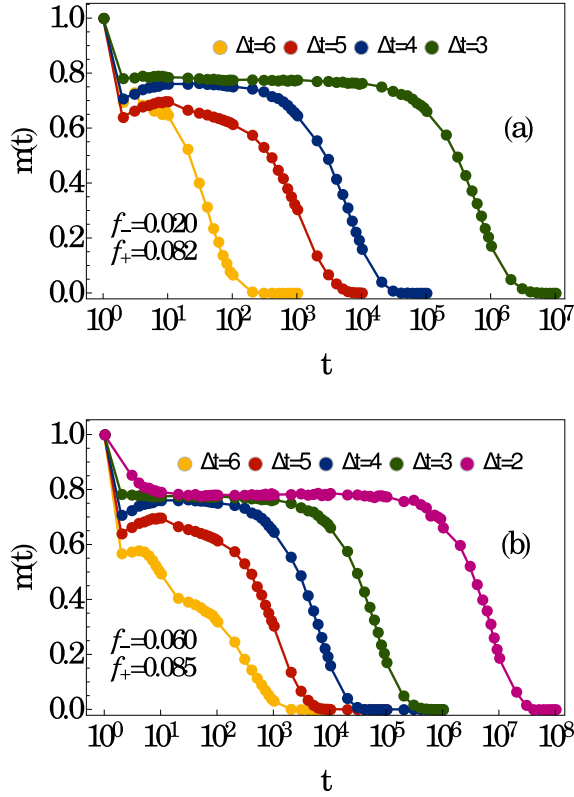
FIG. 3. For a RR network with $k_0 = 12$ and $\theta = 0.45$, (a) and (b) show m averaged over $N_D = 10^3$ realizations for $\Delta t = 2, 3, 4, 5,$ and 6 for $(f_-, f_+) \in$ (ORD,DIS) and (ME,DIS), respectively.

Starting with θ_- and θ_+ belonging to the same phase (ORD and ME and DIS) the resulting phase will be preserved for the temporal disorder, as expected. When θ_- and θ_+ belong to distinct phases, the result phase will depend on the sign of coefficients $A'(f, \theta, k_0)$'s.

The case in which θ_- belongs to ORD and θ_+ belongs to ME/DIS phases, the resulting phase will be or-
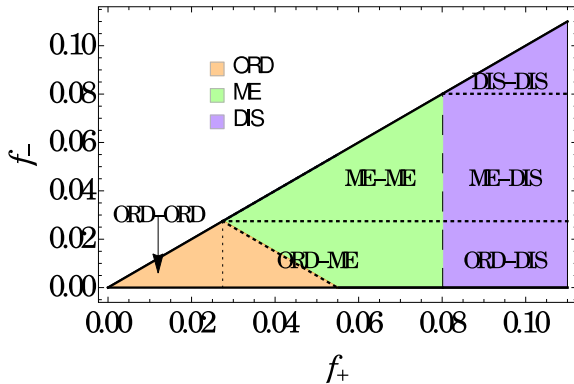

FIG. 4. MFT phase diagram for RR network with values $k_0 = 12$ and $\theta = 0.45$ under temporal disorder over the control parameter f. The resulting phase is represented by distinct colors. Dotted and dashed lines represent crossovers and discontinuous transition lines, respectively.

TABLE I. Coefficients $A'(f, \theta, k_0)$ for $f = 0.12$ and $k_0 = 12$ and the resulting phase.

θ	$A'(f, \theta, k_0)$	Phase
$0 < \theta < 1/7$	$0.614...$	ORD
$1/7 < \theta < 1/4$	$0.467...$	ORD
$1/4 < \theta < 1/3$	$0.192...$	ORD
$1/3 < \theta < 2/5$	$-0.0122...$	ME
$2/5 < \theta < 5/11$	$-0.0979...$	DIS
$5/11 < \theta < 1/2$	$-0.118...$	DIS

dered if $A'(f, \theta_-, k_0) > A'(f, \theta_+, k_0)$ and ME and DIS if $A'(f, \theta_-, k_0) < A'(f, \theta_+, k_0)$, respectively. The competition between θ_- and θ_+ belonging to the ME and DIS phases will also result in the disordered phase. Since both $A'(f, \theta_-, k_0)$ and $A'(f, \theta_+, k_0)$ are negative, the system solely requires a long sequence of $\theta = \theta_+$ for driving it to $m(t) < m_u(\theta_-)$ and then it will evolve to the DIS phase, irrespective of the subsequent values of θ. Although more pronounced for $k_0 = 20$ than for $k_0 = 12$, but (apparently) less pronounced than the disorder in the control parameter, temporal disorder in the inertia is also featured by a long and remarkable period in which the system exhibits ordering until its vanishing [see, e.g., Figs. 5(c) and 6]. As previously, a consecutive sequence of θ_+'s driving the system to the disordered phase also requires larger times for lower Δt's and for this reason the mean time decay $\overline{T}$ increases. A discontinuous phase transition between ME and DIS yields at $\theta_+ = \theta_f$. Thus, the temporal disorder in inertia also does not suppress the existence of a discontinuous transition nor hysteretic branch.

Since the difference between the lowest $A'(f, \theta_-, k_0)$ and the largest $A'(f, \theta_+, k_0)$ is always positive, the ORD phase always prevails over the DIS/ME ones for $k_0 = 12$, $f = 0.12$, and $p = \frac{1}{2}$ [see, e.g., Figs. 5(a) and 5(b)]. The prevalence of the ordered phase over the disordered and metastable phases in such case is a feature originated from the temporal disorder in the inertia, whose main features are exemplified in the phase diagram in Fig. 5(d).

We close this section by mentioning that although not presented for $k_0 = 12$, the competition between ORD and ME and DIS phases can result to a metastable or disordered phase as exemplified for $k_0 = 20$ (see, e.g., coefficients in Table II).

III. BEYOND THE MEAN-FIELD THEORY: MONTE CARLO SIMULATIONS FOR DISTINCT KINDS OF TEMPORAL DISORDER

In this section, we tackle the influence of temporal disorder beyond the MFT by analyzing their effects in complex net-

TABLE II. Coefficients $A'(f, \theta, k_0)$ for $f = 0.12$ and $k_0 = 20$ and the resulting phase.

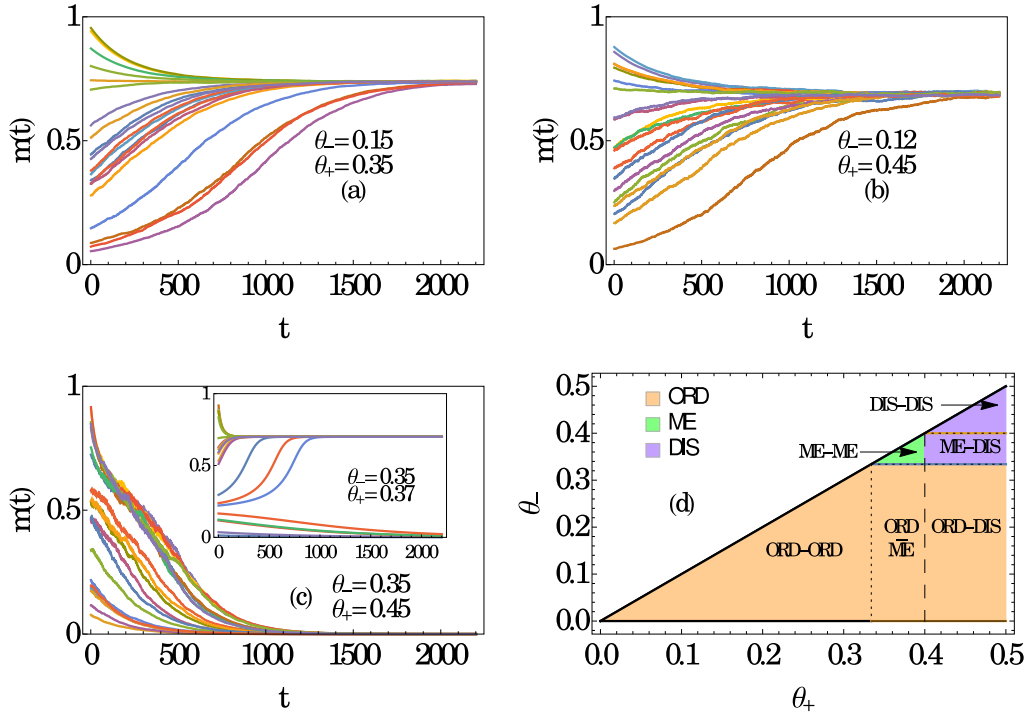| θ	$A'(f, \theta, k_0)$	Phase
$3/13 < \theta < 2/7$	$0.2295...$	ORD
$2/7 \lesssim \theta < 1/3$	$0.0328...$	ORD
$1/3 \lesssim \theta < 3/8$	$-0.0683...$	ME
$3/8$	$-0.0876...$	ME
$3/8 < \theta < 7/17$	$-0.1176...$	DIS

FIG. 5. MFT analysis for the temporal disorder in the inertia: For RR network with values $k_0 = 12$ and $f = 0.12$, (a)–(c) exemplify the average time evolution of the m for distinct initial configurations and sorts of inertia $(\theta_-, \theta_+) \in$: (ORD,ME), (ORD,DIS), (ME,DIS), (ME,ME) (inset), respectively. In (d) the phase diagram with dashed and dotted lines representing discontinuous phase transition lines and crossover between phases, respectively. The resulting phase is represented by distinct colors.

works structures. We also consider random-regular structures which have been built for fixed connectivities k_0 (for a given system size N) according to the scheme by Bollobás [36]. Also, the neighborhood of each site has not been altered as the time is changed.

As in the MFT, numerical simulations start for given initial condition in which a new value of the control parameter (whether f or θ) is sorted from the two possible values (f_-/θ_- and f_+/θ_+) for every interval time ranged between t and $t + \Delta t$. The time evolution of system is analyzed until a maximum time $t_{\max}$ that results in a given sequence of $\{f_1, f_2, \ldots, f_M\}$
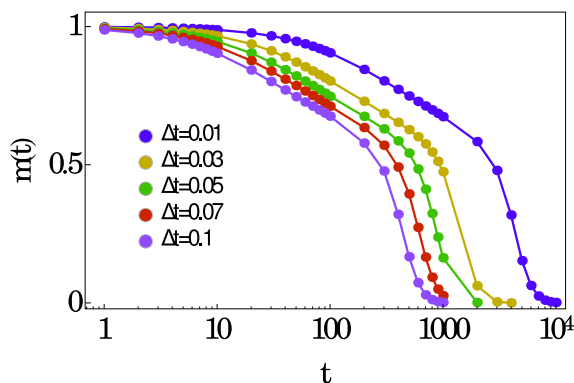

FIG. 6. For $k_0 = 20$, $f = 0.12$, $\theta_- = 0.334 \in$ ME, and $\theta_+ = 0.412 \in$ DIS, the average m versus t obtained for $N_D = 10^3$ disorder realizations and distinct Δt's.

($\{\theta_1, \theta_2, \ldots, \theta_M\}$) in which $t_{\max} = M \times \Delta t$. Such analysis is repeated over $N_D = 10^3 - 10^4$ distinct sequences of temporal disorder. We have considered $\Delta t = 20$ and $t_{\max} = 10^5 - 10^6$.

Resulting phases as well as phase transitions can be identified from two distinct (but equivalent) ways. In the former approach, one considers analysis in the steady-state regime in which we start from the ordered phase ($|m|$ close to 1) and f is raised by an amount Δf and the end configuration at f is adopted as the initial condition at $f + \Delta f$. This procedure is repeated until the system reaches the disordered phase at f_f. Conversely, the numerical simulation is restarted for a given value of f constrained in the disordered phase but now f is decreased by Δf until the ordered phase will be reached at f_b. Both forward and backward curves are expected to coincide themselves at both ordered and disordered phases, but not along the metastable branch.

Additionally, the presence of temporal disorder can be more conveniently analyzed (as previously) by inspecting the time evolution of order parameter for distinct initial conditions $0 < |m(0)| \leqslant 1$. The system will converge for a well defined $m(t \to \infty)$ in both disordered and ordered phases, respectively, irrespective of the initial conditions, whereas it will evolve to two well defined values for f constrained in the metastable branch. Due to the finite-size effects, the magnetization never vanishes, but instead, it behaves as $m(t \to \infty) \sim 1/\sqrt{N}$ in the disordered and metastable phases [for low $m(0)$].

Although the temporal disorder features are not expected to depend on the values of θ and k_0, the bistable branch is more pronounced for large connectivities and θ's and for this reason numerical simulations will be undertaken for $\theta = 0.3$
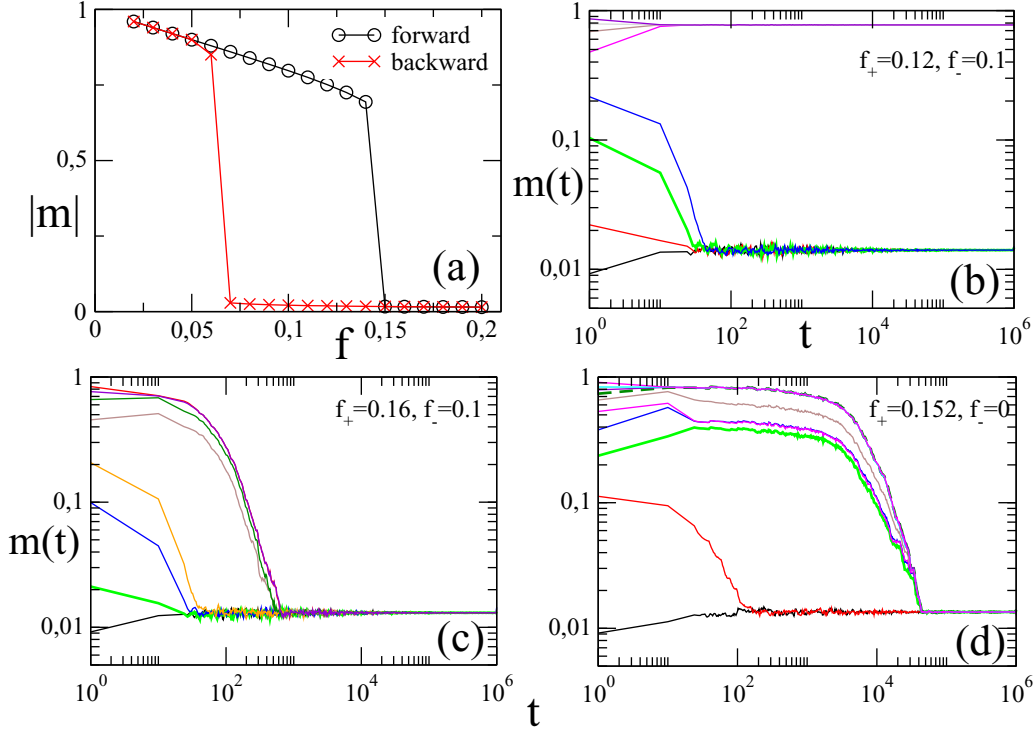
FIG. 7. (a) Depicts, for $N = 5000$, $k_0 = 20$, and $\theta = 0.3$, the order parameter $|m|$ versus f for the pure system. Continuous and dotted lines denote the forward and backward increase of f, respectively. (b)–(d) Show the average time evolution of the order parameter m (over $N_D = 10^4$ realizations) for distinct initial conditions $m(0)$ and different sorts of $[f_-, f_+] \in$ [ME,ME], [ME,DIS], [ORD,DIS]. respectively. Due to finite-size effects, $m(t \to \infty)$ does not vanish in the disorder phase, but it is proportional to $1/\sqrt{N}$.

and $k_0 = 20$, whose hysteretic loop for the pure system was investigated in Ref. [22] and reproduced in Fig. 7(a). As it can be seen, for $f < f_b = 0.060(5)$ the system is constrained in the ordered phase, whereas the bistability yields for $f_b < f < f_f = 0.150(5)$. The disordered phase emerges for $f > f_f$, irrespective of the initial condition. Figures 7(b)–7(d) depict the main features for temporal disorder in the control parameter for distinct sets of f_+ and f_- belonging to the ORD, ME, and DIS phases. In particular, the MFT analysis describes reasonably well the findings obtained from complex topologies, including the prevalence of the disordered phase over the metastable [Fig. 8(a)] for $f_+ < f_f$ and the competition between ordered and metastable and disordered phases. Also, by taking into account that the summation of the lowest $f_- = 0$ and $f_+ = f_f$ is lower than $2f_b$ (for $k_0 = 12$ and $\theta = 0.45$), we can understand (from MFT) the prevalence of the disordered phase over the ORD one, as illustrated in Fig. 5(d). Despite the similarities between MFT and present results, due to a finite-size effects, the ORD phase always prevails over the metastable for finite N. Since $m(t \to \infty)$ is finite and proportional to $1/\sqrt{N}$ in the disordered phase, it suffices a long sequence (e.g., a rare fluctuation) of $f = f_-$ for driving the system to the ORD phase. However, finite-size effects disappear as $N \to \infty$ and MFT also describes well the prevalence of the ME phase when $f_+ + f_- > 2f_b$.

Since the main features are quite similar to those from MFT, we shall omit the phase diagram. As a final comment, we expect similar trends for other lattice topologies, although the line separating ordered and other phases does not necessarily obey a derivation like MFT.

In the last analysis, we exemplify the main features of inertial temporal disorder. Figure 8(b) shows the competition between metastable and disordered phases for $f = 0.12$. For the pure version, the hysteretic branch is verified for $\frac{2}{7} < \theta \leqslant \theta_f = \frac{1}{3}$ in which the order parameter jumps at $\theta > \theta_f$ (see, e.g., [35]).

Also in accordance with previous MFT analysis, the competition between ME and DIS phases always suppresses the phase coexistence [see, e.g., curves for $\theta_+ > \theta_f$ in Fig. 8(b)] and a discontinuous transition yields at $\theta_+ = \theta_f$. On the other hand, the resulting phase from the competition between ORD and DIS phases will depend on particular values of θ_- and θ_+. More specifically, for $\theta_- = 0.28$ and $\frac{1}{3} < \theta_+ = \frac{3}{8}$ the ORD prevails, whereas the system evolves to disordered phase when $\theta_- = 0.29$. Since transition points from MFT and complex topologies are similar for large k_0's [22], the above findings can also be (qualitatively) understood from coefficients from Table II from which the predominance of ORD and DIS phases holds for $\theta_- = 0.28$ and 0.29, respectively.

IV. CONCLUSIONS

Based on the MFT, a general description for discontinuous phase transitions in the presence of temporal disorder was considered. Our theoretical predictions are valid for any system displaying a bistable behavior characterized by the existence of a hysteretic branch. The present study not only confirms previous findings [29], but also extends for other kinds of phase transitions and distinct kinds of temporal disorder. Analysis was exemplified in one of the simplest
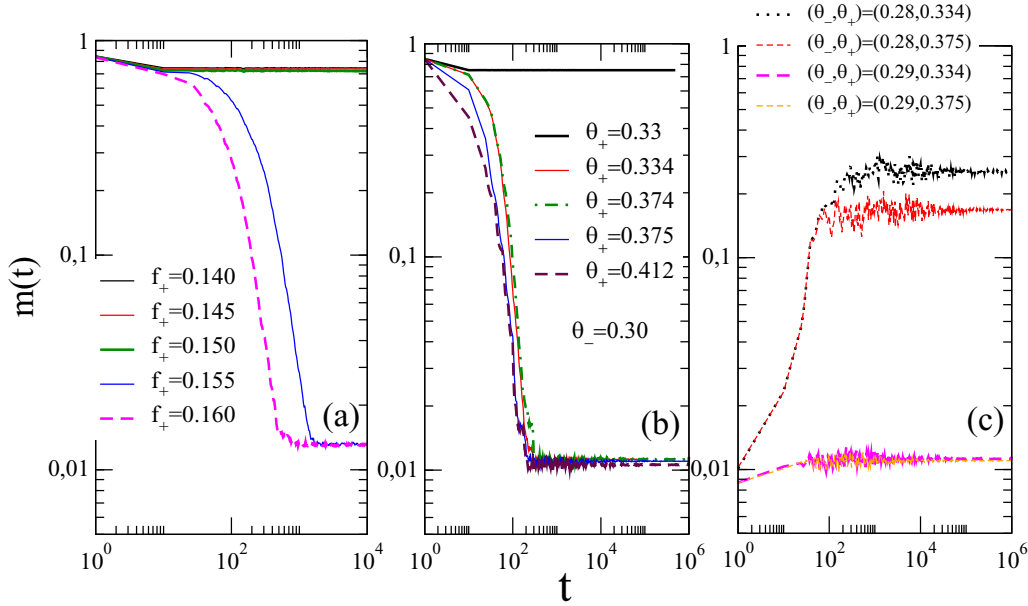
FIG. 8. For a RR network of size $N = 10^4$, $k_0 = 20$, and $\theta = 0.3$, panel (a) depicts the average time evolution of the order parameter m starting from the ordered state for $f_- = 0.10$ (ME) for distinct f_+'s. (b) Depicts, for $f = 0.12$ and $m(0) = 1$, the time evolution of the average m for $\theta_- = 0.30$ (ME) for distinct θ_+'s. In (c) the same but for $\theta_- = 0.28$ and 0.29 (both belonging to the ORD phase) and distinct θ_+'s starting from $m(0) = 10^{-4}$. In all cases, averages are evaluated over $N_D = 10^3$–10^4 realizations. Due to finite-size effects, $m(t \to \infty)$ does not vanish in the disorder phase, but it is proportional to $1/\sqrt{N}$.

"up-down" Z_2 symmetry for two kinds of temporal disorder: the inertial majority vote model. Since the inertia plays a fundamental role for the emergence of a discontinuous transition, the effect of its time variation was also investigated. Although both kinds of temporal disorder do not suppress existence of a discontinuous phase transition, the phase coexistence is always suppressed when there is a competition between disordered and metastable phases. As for APTs, the competition between different phases can also lead to an order-parameter vanishing characterized by exponentially large decay times.

The mean-field approach describes very well the effect of temporal disorder in complex topologies and one expects its validity for other complex networks, such as Erdös-Renyi and heterogeneous structures. As a final comment, it will be remarkable to extend such analysis for discontinuous phase transitions in regular structures, which presents an entirely different behavior from complex topologies. In these systems, no hysteretic behavior is presented [27,28].

[1] J. Marro and R. Dickman, *Nonequilibrium Phase Transitions in Lattice Models* (Cambridge University Press, Cambridge, 1999).

[2] M. Henkel, H. Hinrichsen, and S. Lubeck, *Non-Equilibrium Phase Transitions Volume I: Absorbing Phase Transitions* (Springer, The Netherlands, 2008).

[3] G. Ódor, *Universality In Nonequilibrium Lattice Systems: Theoretical Foundations* (World Scientific, Singapore, 2007).

[4] T. Vojta and M. Dickison, Phys. Rev. E **72**, 036126 (2005).

[5] T. Vojta and M. Y. Lee, Phys. Rev. Lett. **96**, 035701 (2006).

[6] M. M. de Oliveira and S. C. Ferreira, J. Stat. Mech (2008) P11001.

[7] T. Vojta, A. Farquhar, and J. Mast, Phys. Rev. E **79**, 011111 (2009).

[8] H. Barghathi and T. Vojta, Phys. Rev. Lett **109**, 170603 (2012).

[9] F. Vazquez, J. A. Bonachela, C. López, and M. A. Muñoz, Phys. Rev. Lett. **106**, 235702 (2011).

[10] R. Martínez-García, F. Vazquez, C. López, and M. A. Muñoz, Phys. Rev. E **85**, 051125 (2012).

[11] J. A. Hoyos and T. Vojta, Europhys. Lett. **112**, 30002 (2015).

[12] T. Vojta and R. Dickman, Phys. Rev. E **93**, 032143 (2016).

[13] H. Barghathi, T. Vojta, and J. A. Hoyos, Phys. Rev. E **94**, 022111 (2016).

[14] C. M. D. Solano, M. M. de Oliveira, and C. E. Fiore, Phys. Rev. E **94**, 042123 (2016).

[15] M. M. de Oliveira and C. E. Fiore, Phys. Rev. E **94**, 052138 (2016).

[16] A. H. O. Wada, M. Small, and T. Vojta, Phys. Rev. E **98**, 022112 (2018).

[17] Alexander H. O. Wada and José A. Hoyos, Phys. Rev. E **103**, 012306 (2021).

[18] O. Al Hammal, H. Chaté, I. Dornic, and M. A. Muñoz, Phys. Rev. Lett. **94**, 230601 (2005).

[19] C. Castellano, S. Fortunato, and V. Loreto, Rev. Mod. Phys. **81**, 591 (2009).

[20] T. Vicsek and A. Zafeiris, Phys. Rep. **517**, 71 (2012).

[21] J. A. Acebrón, L. L. Bonilla, C. J. P. Vicente, F. Ritort, and R. Spigler, Rev. Mod. Phys. **77**, 137 (2005).

[22] H. Chen, C. Shen, H. Zhang, G. Li, Z. Hou, and J. Kurths, Phys. Rev. E **95**, 042304 (2017).

[23] M. J. de Oliveira, J. Stat. Phys. **66**, 273 (1992).

[24] H. Chen, C. Shen, G. He, H. Zhang, and Z. Hou, Phys. Rev. E **91**, 022816 (2015).

[25] L. F. C. Pereira and F. G. Brady Moreira, Phys. Rev. E **71**, 016123 (2005).

[26] P. E. Harunari, M. M. de Oliveira, and C. E. Fiore, Phys. Rev. E **96**, 042305 (2017).

[27] J. M. Encinas, P. E. Harunari, M. M. de Oliveira, and C. E. Fiore, Sci. Rep. **8**, 9338 (2018).

[28] M. M. de Oliveira, M. G. E. da Luz, and C. E. Fiore, Phys. Rev. E **97**, 060101(R) (2018).

[29] C. E. Fiore, M. M. de Oliveira, and J. A. Hoyos, Phys. Rev. E **98**, 032129 (2018).

[30] P. Villa Martín, J. A. Bonachela, and M. A. Muñoz, Phys. Rev. E **89**, 012145 (2014).

[31] P. Grassberger, J. Stat. Mech. (2006) P01004.

[32] S. Lubeck, J. Stat. Phys. **123**, 193 (2006).

[33] C. E. Fernandéz Noa, P. E. Harunari, M. J. de Oliveira, and C. E. Fiore, Phys. Rev. E **100**, 012104 (2019).

[34] C. Castellano and R. Pastor-Sartorras, J. Stat. Mech. (2006) P05001.

[35] J. M. Encinas, H. Chen, M. M. de Oliveira, and C. E. Fiore, Phys. A (Amsterdam) **516**, 563 (2019).

[36] B. Bollobás, Eur. J. Combin. **1**, 311 (1980).